

The Telomerase Inhibitor Imetelstat Depletes Cancer Stem Cells in Breast and Pancreatic Cancer Cell Lines

Immanuel Joseph¹, Robert Tressler¹, Ekaterina Bassett¹, Calvin Harley¹, Christen M. Buseman², Preeti Pattamatta¹, Woodring E. Wright², Jerry W. Shay², and Ning F. Go¹

Abstract

Cancer stem cells (CSC) are rare drug-resistant cancer cell subsets proposed to be responsible for the maintenance and recurrence of cancer and metastasis. Telomerase is constitutively active in both bulk tumor cell and CSC populations but has only limited expression in normal tissues. Thus, inhibition of telomerase has been shown to be a viable approach in controlling cancer growth in nonclinical studies and is currently in phase II clinical trials. In this study, we investigated the effects of imetelstat (GRN163L), a potent telomerase inhibitor, on both the bulk cancer cells and putative CSCs. When breast and pancreatic cancer cell lines were treated with imetelstat *in vitro*, telomerase activity in the bulk tumor cells and CSC subpopulations were inhibited. Additionally, imetelstat treatment reduced the CSC fractions present in the breast and pancreatic cell lines. *In vitro* treatment with imetelstat, but not control oligonucleotides, also reduced the proliferation and self-renewal potential of MCF7 mammospheres and resulted in cell death after <4 weeks of treatment. *In vitro* treatment of PANC1 cells showed reduced tumor engraftment in nude mice, concomitant with a reduction in the CSC levels. Differences between telomerase activity expression levels or telomere length of CSCs and bulk tumor cells in these cell lines did not correlate with the increased sensitivity of CSCs to imetelstat, suggesting a mechanism of action independent of telomere shortening for the effects of imetelstat on the CSC subpopulations. Our results suggest that imetelstat-mediated depletion of CSCs may offer an alternative mechanism by which telomerase inhibition may be exploited for cancer therapy. *Cancer Res*; 70(22); 9494–504. ©2010 AACR.

Introduction

Tumors have a hierarchical arrangement of cell populations with different biological properties (1, 2). Similar to resident adult stem cells in tissues, tumors have rare cell subpopulations with stem-like properties that are called cancer stem cells (CSC). The characteristics that define CSCs include self-renewal, clonogenic and tumorigenic potential, transient quiescence, which are believed to contribute to CSCs resistance to conventional therapies, and asymmetrical division. The resulting daughter cell retains the CSC phenotype, whereas the second daughter cell proliferates and reconstitutes the bulk of the tumor mass. CSCs are key to sustaining tumor growth, recurrence, and metastasis (3–6).

CSCs were initially identified in acute myeloid leukemia and have since been identified in other hematologic malignancies and a variety of solid tumors including brain, breast, pancreatic, prostate, colon, ovarian cancers, and melanoma (1, 7). A single CSC may, theoretically, be able to reestablish an entire tumor (8). Many investigators have shown that the number of CSCs needed to establish xenograft tumors in immunocompromised mice is significantly lower than the number of bulk tumor cells required (6, 9). Because CSCs can be quiescent and frequently have multiple drug resistance pathways (10), standard treatment regimens that are effective at targeting the bulk tumor population may not eradicate resistant CSCs, resulting in tumor recurrence and metastasis (3, 11). Hence, therapies that target CSCs are essential for an efficacious and durable response in cancer treatment (12).

A key characteristic of the cancer cell is its immortal phenotype, and in the great majority of cancers, the enzyme telomerase is critical for maintaining the infinite replicative potential of a cancer cell. Normal adult tissues typically do not express telomerase and do not possess an immortal phenotype, suggesting that telomerase is a promising therapeutic target for the treatment of a broad range of tumor types (13). In the absence of active telomerase, telomeres will shorten at each cell division. When the telomeres reach a critically short length, chromosomal instability, cell senescence, and apoptosis are triggered (14, 15). In the majority of fast growing tumors, telomeres are

Authors' Affiliations: ¹Geron Corporation, Menlo Park, California and ²Department of Cell Biology, University of Texas Southwestern Medical Center, Dallas, Texas

Note: Supplementary data for this article are available at Cancer Research Online (<http://cancerres.aacrjournals.org/>).

Current address for C. Harley: Telome Health Inc., Menlo Park, CA 94025.

Corresponding Authors: Ning Go or Immanuel Joseph, Geron Corporation, 200 Constitution Drive, Menlo Park, CA 94025. Phone: 650-566-7130; Fax: 650-473-7760; E-mail: ijoseph@geron.com or ngo@geron.com.

doi: 10.1158/0008-5472.CAN-10-0233

©2010 American Association for Cancer Research.

stabilized through reactivation of telomerase. Inhibition of telomerase has been shown to limit the growth of cancer cells in multiple tumor types (16–19). Both bulk cancer cells and CSCs express telomerase, although the level of telomerase activity and/or the telomere length observed in CSCs relative to their bulk tumor counterpart have been reported to vary with tissue type (4, 20–22). It has been suggested that CSCs could be sensitive to telomerase-based therapy (23).

Imetelstat sodium is a 5' palmitoylated 13-mer thiophosphoramidate oligonucleotide, composed of the sequence 5'-TAGGGTTAGACAA-3', complementary to the template region of human telomerase RNA component (hTR). It acts as a highly specific and potent competitive inhibitor of telomeric repeat addition (22, 24). The IC_{50} s for telomerase inhibition ranges from 0.1 to 1 μ mol/L in most tumor cell lines tested. *In vitro* treatment of tumor cell lines with imetelstat results in progressive telomere shortening leading to cell senescence or apoptosis (18, 19). *In vivo* treatment with imetelstat in xenograft models results in the inhibition of tumor growth and metastasis (17–20, 25). Recently, Marian and colleagues showed that imetelstat targets primary human glioblastoma tumor-initiating cells, leading to decreased tumor growth (20). Imetelstat has shown efficacy against bulk tumor cell populations as a single agent, as well as having synergistic antitumor activity when combined with Herceptin, paclitaxel, or radiation treatment in breast cancer models *in vitro* and *in vivo* (26, 27). Imetelstat is currently in phase II clinical development for breast cancer, non-small cell lung carcinoma, multiple myeloma, and other tumor types (13).

In this study, we tested the effect of imetelstat on putative CSC populations present in PANC1, MDA-MB231, and MCF7 cell lines. We enriched for CSCs from the MCF7 line by mammosphere culture and investigated the effect of imetelstat on telomerase activity, self-renewal potential, and cell proliferation. PANC1 and MDA-MB231 monolayers were treated with imetelstat and evaluated for CSC depletion and effects on tumorigenicity *in vivo*. The relationship between imetelstat effects, telomerase activity, and telomere length were also studied to explore the mechanistic basis of the effect of imetelstat on CSCs.

Materials and Methods

Cell culture, media, and drug treatment

MCF7 monolayer cells were maintained in RPMI 1640 containing 10% fetal bovine serum (FBS). Monolayer MDA-MB231 and PANC1 cells were maintained in DMEM/F12 containing 20% FBS. MCF7 mammospheres were maintained by culturing cells in ultralow adhesion plates (Corning 3417 and 3814) in the CSC media (DMEM/F12 containing 5 ng/ μ L insulin, 20 ng/mL epidermal growth factor, 10 ng/mL basic fibroblast growth factor, and 0.4% insulin; ref. 4). Subculture of mammospheres was done by incubating mammospheres for 7 minutes at 37°C with 0.25% trypsin/EDTA and reseeding

in fresh CSC media. All treatments with imetelstat were at a final concentration of 10 μ mol/L, unless noted otherwise. Imetelstat was replenished at each cell passage. For monolayer cultures, cells were allowed to attach before adding imetelstat. Imetelstat, 5'-palm-TAGG-GTTAGACAA-3', mismatch control 5'-palm-TAGGTG-TAAGCAA-3' (GRN140833), and sense strand control 5'-palm-TGTCTAACCTA-5' were synthesized at Geron Corporation.

Fluorescence-activated cell sorting analysis and cell sorting

Flow cytometric analysis was performed using FACSCalibur (BD Biosciences). The CSC markers were previously published (28–31). Cell sorting was performed using FACSARIA (BD Biosciences). Antibodies used for putative CSC surface markers were PerCP-Cy5.5-conjugated anti-mouse/human CD44, phycoerythrin (PE)-conjugated mouse anti-human CD24 (BD Biosciences), PE-conjugated CD138 (BD Biosciences), FITC-conjugated anti-EpCAM (BD Biosciences), and PE-conjugated mouse IgG2a isotype control (eBiosciences).

Aldehyde dehydrogenase activity assay

Aldehyde dehydrogenase-positive (ALDH+) cells were quantitated using the Aldefluor kit (StemCell Technologies) as per manufacturer's instructions.

Telomerase activity assay

The telomeric repeat amplification protocol assay was performed as previously described (32) with minor modifications. In some experiments, the use of the internal control primer (TSU2) was eliminated to reduce competitive interference.

Telomere length assay

XpYp single-telomere length amplification (XpYp STELA) assays were performed as per the method described by Baird and colleagues (33) and Xu and Blackburn (34). STELA is a PCR-based single-telomere amplification and Southern blot hybridization technique that allows evaluation of single-telomere lengths (33). The TeloTAGGG telomere length assay kit (Roche) was used to detect the telomere sequence on the gel. To better assess imetelstat's effect on telomere length, a modified universal STELA, which determines telomere length of all chromosome ends present in a cell, was used (35). In brief, new linkers were designed, and assay conditions were optimized to obtain a representative telomere length distribution and average telomere length measurement.

Self-renewal assay

The assay was performed by plating a single MCF7 cell per well in 96-well plates in CSC medium. Wells were marked for the presence of a single cell. After 3 weeks, the wells containing single cells after seeding were scored for sphere formation. Self-renewal potential was calculated as the percentage of single cells that formed spheres.

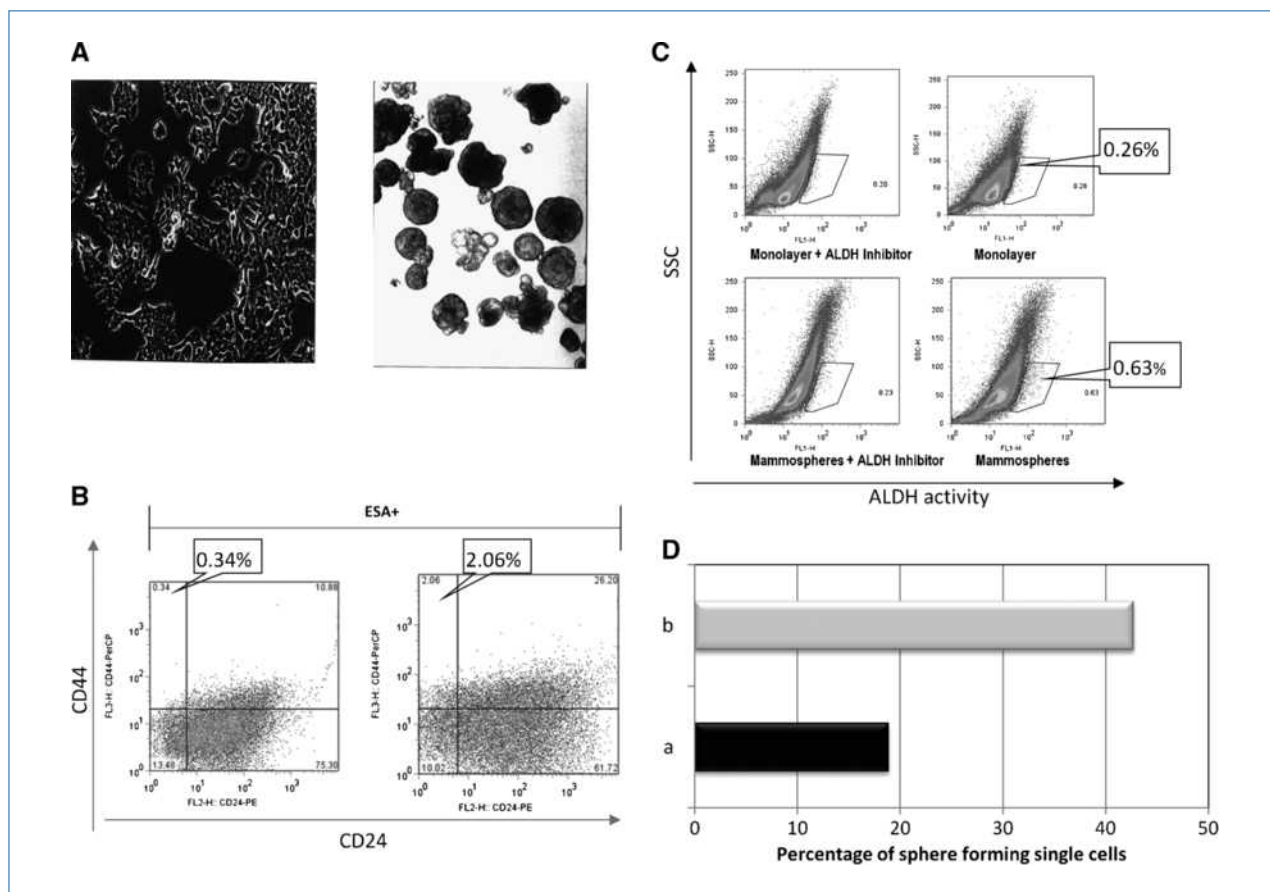


Figure 1. A, MCF7 cells were grown as a monolayer or as mammospheres. Mammospheres could be serially passaged for at least 3 mo. B, MCF7 mammosphere cultures showed an increased frequency of CD44+/CD24⁻/ESA⁺ CSCs relative to monolayer cultures. C, the percentage of Aldefluor-positive cells was increased in MCF7 mammospheres relative to monolayer cultures. D, frequency of self-renewing cells was higher in the mammospheres (light color bar, 42%) than in the monolayer cells (dark color bar, 19%).

Mammosphere growth

Monolayer MCF7 cells were seeded in 96-well plates at a single cell per well in CSC medium. After 4 weeks, mammospheres were harvested, and the total number of cells was counted to quantify mammosphere growth.

Xenograft studies

Xenograft studies were performed according to the guidelines of Geron's Institutional Animal Care and Use Committee. Tumor cells (0.5×10^6) per mouse were injected s.c. in Hsd nude mice (Harlan Laboratories). Animals were treated with saline vehicle or imetelstat posttumor implantation at 30 mg/kg, thrice weekly, i.p. The percentage of animals developing tumors was recorded, and tumor volumes were determined in some studies.

Results

CSC determinations in breast and pancreatic cancer cell lines

Using conditions previously reported (4), MCF7 mammospheres were cultured in CSC medium. MCF7 mammo-

spheres grew robustly from single cells and could be continuously subcultured for at least up to 3 months (Fig. 1A). Using CD44+/CD24⁻/ESA⁺ as breast CSC cell surface markers, the percentage of putative CSCs in MCF7 monolayer ranged from 0.34% to 0.82% of the total cell population (Fig. 1B). Culturing MCF7 cells as mammospheres significantly increased the CD44+/CD24⁻/ESA⁺ population by up to 6-fold (χ^2 test, $P < 0.0001$; Fig. 1B). Mammospheres also showed a 2.7-fold increase in Aldefluor-positive cells compared with monolayer cells (0.63% versus 0.26%, respectively; Fig. 1C). Using the self-renewal assay, 23 of 245 single cells (9.3%) from a MCF7 monolayer cell culture were clonogenic (defined as forming new clones). In contrast, 106 of 248 (42.7%) single cells from MCF7 mammosphere cultures were clonogenic (Fig. 1D; Fisher's exact test, $P < 0.0001$). This is consistent with cell surface marker measurements showing that the percentage of CSCs from the MCF7 line was greater in mammospheres than in monolayer culture. To assess the effect of long-term mammosphere culture on the maintenance of CSC phenotypes, we sorted CD44+/CD24⁻/ESA⁺ cells to >62% purity and seeded the enriched CSCs back into mammosphere

culture. Fluorescence-activated cell sorting (FACS) analysis 4 weeks later showed that the percentage of CD44+/CD24-/ESA+ cells reverted to presorting levels during this time (Supplementary Fig. S1), supporting the possibility of asymmetrical division in CSCs (36) or cell differentiation into more mature phenotypes.

Imetelstat treatment results in telomerase inhibition and telomere shortening

Treatment with imetelstat at 10 $\mu\text{mol/L}$ significantly inhibited telomerase activity in all three cell lines tested [MCF7 (94.6% inhibition, *t* test, $P < 0.0001$), PANC1 (93.5% inhibition, *t* test, $P = 0.005$), and MDA-MB 231 (87% inhibition, *t* test, $P = 0.0002$; Fig. 2A–C) without major effect on cell growth rates. Sense strand negative control oligonucleotide did not inhibit telomerase (Fig. 2D). To investigate whether telomerase inhibition leads to telomere shortening in imetelstat-treated cells, we measured telomere length using the XpYp STELA assays. To assess telomere shortening in treated and untreated samples, the total number of single telomere bands in six gel lanes were counted for each sample

and the percentage of those under 2, 3, or 4 kb were plotted. Telomere shortening occurred in the imetelstat-treated MCF7 mammospheres compared with untreated controls (Supplementary Fig. S2B). Similar trends in the reduction of telomere length were observed in MCF7 and PANC1 monolayer cells following imetelstat treatment (Supplementary Fig. S2A and C).

Imetelstat treatment results in depletion of CSCs in breast and pancreatic cell lines

MCF7 mammospheres were treated with imetelstat continuously for ~ 3.5 weeks, and at the end of treatment, CSC surface markers were evaluated. Imetelstat treatment reduced the proportion of CD44+/CD24-/ESA+ cells in mammospheres from 2% to 0.16% (Fig. 3A; Fisher's exact test, $P < 0.0001$). Similar results were noted in PANC1 monolayer cells treated with imetelstat for 7 weeks. Imetelstat treatment depleted the CD44+/CD24-/ESA+ population in PANC1 cells, leading to a >3 -fold (7.7–2%) reduction by 7 weeks (Fig. 3B; ANOVA, $P = 0.012$). In a repeat experiment, PANC1 cells treated with imetelstat for 5 weeks showed a

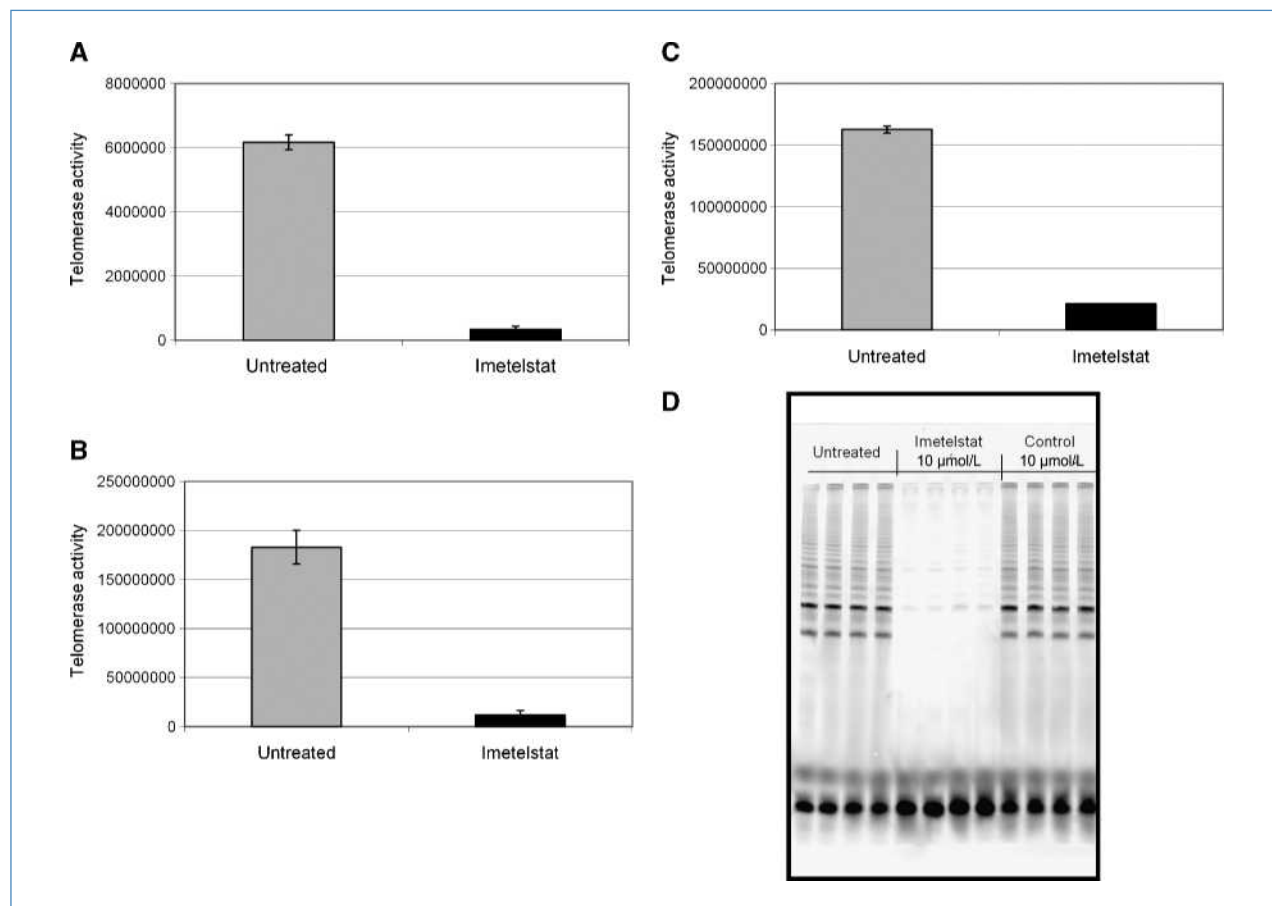


Figure 2. Imetelstat inhibited telomerase activity in all three cell lines tested: (A) MCF7 mammospheres ($n = 3$, measured at 12 d of treatment), (B) PANC1 monolayers ($n = 2$, measured at 45 d of treatment), and (C) MDA-MB231 ($n = 2$, measured at 49 d of treatment). D, imetelstat, but not the sense strand control (GRN140832), inhibited telomerase activity in MCF7 mammospheres (each lane represents a separate treatment sample).

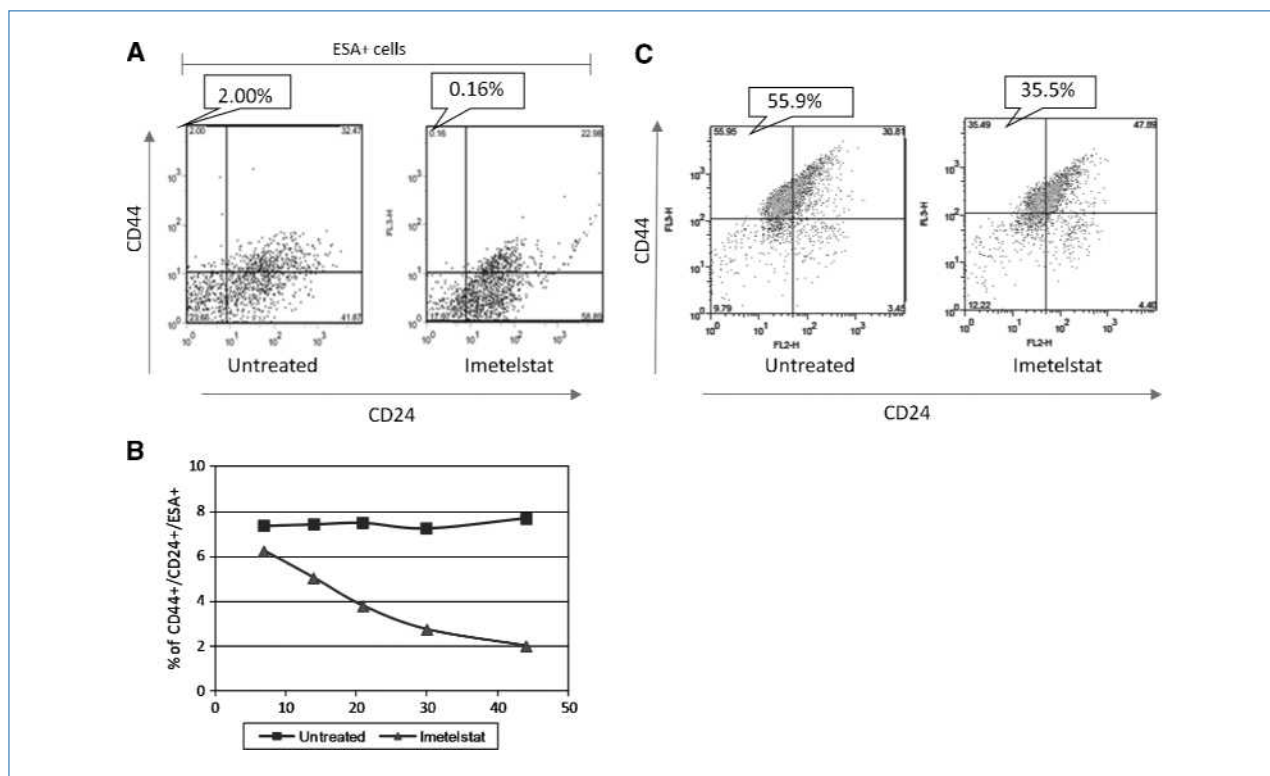


Figure 3. Imetelstat treatment reduced the percentage of CSCs in MCF7, MDA-MB231, and PANC1 cells. A, imetelstat treatment reduced the numbers of CD44+/CD24-/ESA+ cells in MCF7 mammospheres. B, percentage of ESA+/CD24+/CD44+ pancreatic CSCs was assessed weekly in the untreated and imetelstat-treated PANC1 cells. Cells expressing CSC markers decreased from ~7% to 2% over the course of 6.5 wk of treatment. C, imetelstat treatment reduced percentage of cells expressing CD44+/CD24_{low} CSCs in MDA-MB231 cells. For all FACS analyses, 20,000 cells were acquired. Gating was based on the isotype control antibody or where the antibodies were directly conjugated based on the profiles of the stain-negative cells.

>2-fold reduction in the CD44+/CD24-/ESA+ population (data not shown). MDA-MB231 monolayer cells treated with imetelstat for 47 days likewise showed a reduction in the CD24-/low/CD44+ population (1.6-fold and 2.7-fold in two independent experiments; Fig. 3C; Fisher's exact, $P < 0.0001$). To assess the effect of CSC depletion in a functional assay, we measured changes in ALDH+ cells after imetelstat treatment. The percentage of ALDH+ PANC1 cells was reduced 1.1-fold to 2.2-fold in three independent assays (representative result in Supplementary Fig. S4A). This was reproduced in MDA-MB231 cells (Supplementary Fig. S4B). In summary, our results show that imetelstat treatment depletes CSC cells from bulk tumor populations in three tumor cell lines, as monitored by ALDH positivity and CSC marker expression.

Long-term imetelstat treatment results in cell growth inhibition and cell death

The effect of imetelstat on cell growth of MCF7 mammospheres was compared with untreated, mismatch, or sense strand controls. Imetelstat-treated MCF7 mammospheres showed a significant decrease in the cumulative population doublings (Δ PD) over 3.5 weeks compared with untreated cultures (ANOVA, $P < 0.0001$; Fig. 4A). Imetelstat-treated MCF7 mammospheres underwent cell death after 3 weeks,

and the majority of cells were nonviable at the end of 4 weeks of treatment (Fig. 4A; Supplementary Fig. S4). Mammospheres treated with mismatch or sense strand control oligonucleotides showed only a slight decrease in population doublings (Fig. 4A). Imetelstat effect on cell proliferation and viability became apparent within 2 weeks of treatment. This is faster than it would be expected if telomere shortening were the sole cause of cell apoptosis or death. The onset of viability changes with imetelstat also argues against an acute nonspecific toxicity related to treatment. Mammospheres treated with imetelstat at 3 μ mol/L had a reduced effect on Δ PD relative to treatment with 10 μ mol/L (data not shown). A less dramatic but statistically significant effect on Δ PD was observed with monolayer MCF7 cells treated with 10 μ mol/L imetelstat (ANOVA, $P = 0.0088$; Fig. 4B).

Imetelstat treatment decreases self-renewal and sphere growth of MCF7 CSCs

The ability of a single breast cancer cell to give rise to an anchorage-independent sphere of cells is a key stem-like characteristic. To test the effect of imetelstat on the self-renewal potential of CSCs, MCF7 mammospheres were pretreated with imetelstat for 3 weeks and single cells derived from the treated mammospheres were plated into

96-well plates. The percentage of single cells that gave rise to a clonal mammosphere was calculated. Imetelstat treatment significantly reduced the frequency of self-renewing MCF7 mammospheres by >2-fold, from 42% to 19% (Fig. 4C; Fisher's exact test, $P = 0.0064$). To rule out the possibility that the reduction in self-renewing cells was an artifact of the prolonged mammosphere culture, we treated the MCF7 monolayer cells with imetelstat for up to 2 months and seeded the cells in CSC medium. Mammosphere growth was measured by cell counts. Imetelstat-treated MCF7 cells also showed a dramatic reduction in the ability to grow as mammospheres. The number of cells in the spheres was reduced >7.8-fold in the imetelstat-treated groups compared with untreated control (Fig. 4D). These results show that imetelstat treatment inhibits the ability of MCF7 cells to grow as mammospheres and their self-renewal potential.

Imetelstat treatment decreases the *in vivo* tumorigenicity of PANC1 and MDA-MB231 cells

To provide further evidence that imetelstat treatment depletes CSCs from bulk tumor cells, tumor engraftment xenograft studies were performed. PANC1 cells were pretreated *in vitro* with imetelstat for 45 days until the per-

centage of CD44⁺/CD24⁺/ESA⁺ cells was reduced >3-fold compared with the untreated control. Five million untreated or pretreated PANC1 cells were implanted s.c. in nude mice. Animals receiving untreated PANC1 cells were treated with saline *in vivo* (Group 1). Animals receiving imetelstat-pretreated PANC1 cells were treated with saline or with additional imetelstat at 30 mg/kg, thrice weekly, for 6.5 weeks (groups 2 and 3, respectively). The percentage of implanted animals that developed tumors was recorded for 6.5 weeks. The tumor engraftment rate was 100% for group 1 at day 46, 50% for group 2, and 40% for group 3 (Fig. 5A). These results were reproduced in an independent experiment (data not shown). The reduction in tumorigenicity was statistically significant relative to the untreated group in both studies (study 1, ANOVA, $P = 0.0098$; study 2, ANOVA, $P = 0.0011$). The finding was further confirmed in the MDA-MB231 model. Implantation of untreated MDA-MB231 cells resulted in an 80% tumor engraftment rate on day 50. Whereas the imetelstat-pretreated group had the same tumor take rate as the control group, maximal engraftment had a lag time of 3 weeks compared with the untreated control group. The group that received both imetelstat *in vitro* pretreatment and postimplantation

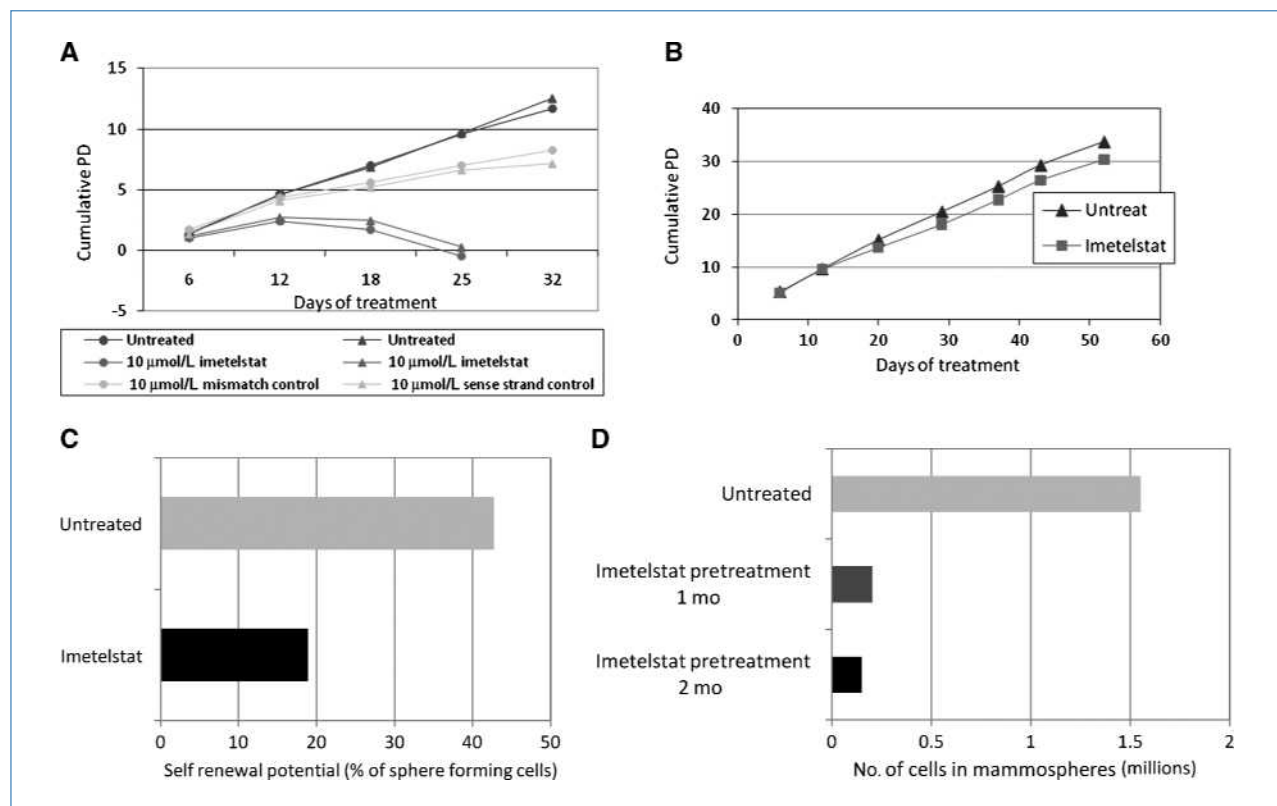


Figure 4. Imetelstat treatment inhibited mammosphere cell growth and cell self-renewal potential. A, MCF7 mammosphere growth was measured at each passage up to 32 d. Growth inhibition was measured by population doublings. Growth of two cultures each of untreated and 10 μmol/L imetelstat treatment and one culture each of sense and mismatch oligonucleotides. B, treatment of MCF7 monolayer with imetelstat caused a small but significant reduction in proliferation. C, MCF7 mammosphere cells were pretreated with imetelstat, and self-renewal potential was measured by the sphere growth from single cells. D, in a similar assay, MCF7 monolayer cell self-renewal potential was assayed.

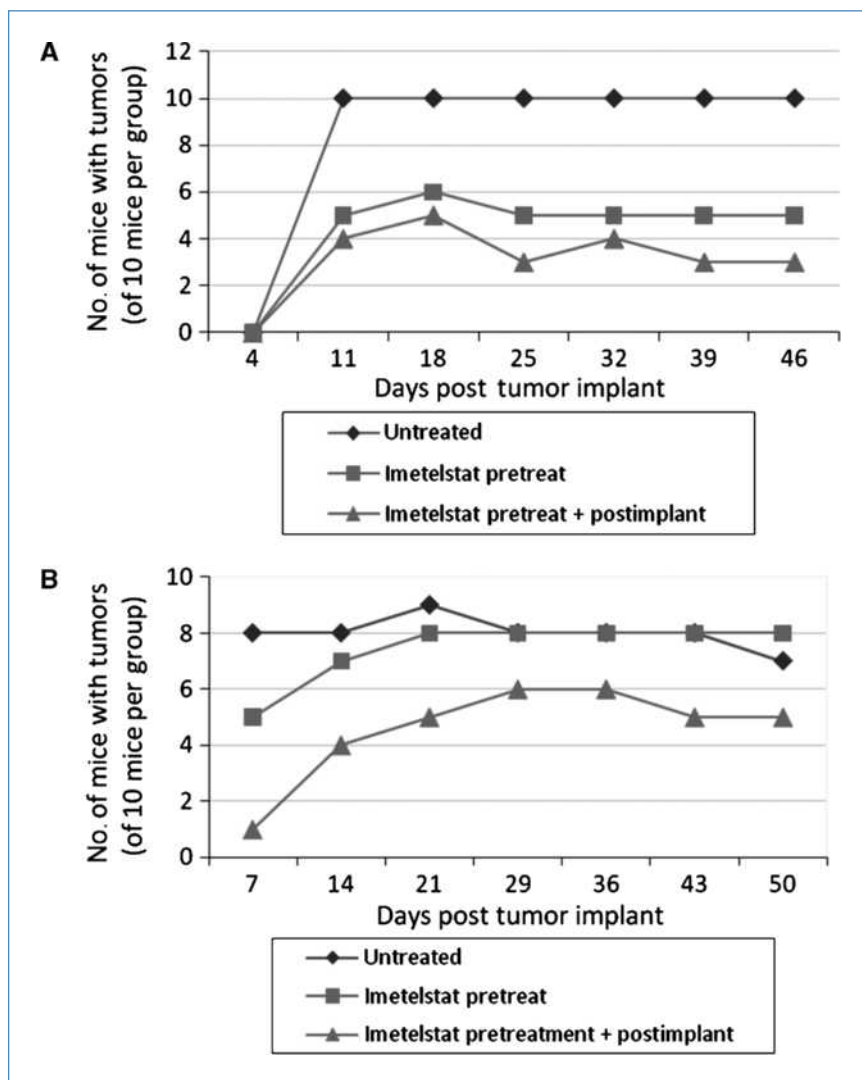


Figure 5. Imetelstat-pretreated PANC1 and MDA-MB231 cells showed reduced tumorigenicity in xenograft models. A, PANC1 xenograft tumor take rate was scored up to day 46 ($n = 10$ per group). B, MDA-MB231 xenograft tumor take rate was scored up to day 50.

in vivo treatment had a reduced tumor take rate of 50% by day 50 (ANOVA, $P = 0.0048$; Fig. 5B).

Absence of differences in patterns of telomerase activity or telomere length between CSCs and bulk tumor cells

To understand the reason for the difference in susceptibility of CSCs and bulk tumor cells to imetelstat, baseline telomerase activity and telomere length were compared between CSC and bulk tumor cell subpopulations in PANC1, MDA-MB231, MCF7, and a multiple myeloma cell line, RPMI8226. CSCs were sorted based on their respective CSC surface markers. No consistent pattern in the levels of telomerase activity between CSC and non-CSC cells in MDA-MB231, MCF7, PANC1, and RPMI8226 cell lines was observed. For example, the sorted CSCs from MDA-MB231 (CD44+/CD24 low) and RPMI-8226 (CD138-) cell lines had lower telomerase activities than bulk tumor cell populations

(CD44-/CD24 high and CD138+, respectively; Fig. 6A and B). However, in the sorted PANC1 CSCs (CD44+/CD24+/ESA+), telomerase activity was higher than their non-CSC (CD44-/CD24-/ESA-) counterparts (Fig. 6C). Similarly, telomerase activity of MCF7 mammospheres was lower than that of the MCF7 monolayer cells they were derived from (Fig. 6D). These findings are consistent with those of Brenman and colleagues (37), wherein they showed that CSC telomerase activity varied among cell lines and from patient to patient.

To compare telomere length, we used XpYp STELA, which measures XpYp telomere length in a cell, or universal STELA, measuring all telomere length in a cell. Results from the universal STELA assays failed to show a significant difference in the telomere lengths between CSC and bulk tumor cell populations from PANC1, MDA-MB231, or RPMI8226 cell lines (Fig. 7). A higher proportion of short telomeres was detected in MCF7 mammospheres relative

to MCF7 monolayer cells by the XpYp STELA assay (Supplementary Fig. S5). There was no consistent pattern of differences in telomerase activity or telomere lengths between sorted CSCs and non-CSCs in PANC1, MDA-MB231, and RPMI8226 cell lines, and thus, the increased sensitivity of CSCs to imetelstat could not be explained by telomerase activity or telomere length differences between CSC and bulk tumor cells.

Discussion

In this study, we showed that imetelstat inhibited telomerase activity and reduced telomere length in MCF7 and MDA-MB231 breast cancer as well as PANC1 pancreatic cancer cell lines. Imetelstat treatment decreased the per-

centage of CSCs in the bulk tumor population, as shown by the reduction of CSC surface marker-bearing populations and ALDH⁺ cells. Long-term imetelstat treatment diminished the self-renewal potential of MCF7 cells, leading to inhibition of mammosphere growth and cell death. The reduction in CSC numbers was accompanied by a decrease in the tumorigenic potential of PANC1 and MDA-MB231 cells in xenograft models *in vivo*.

These results are the first to show that telomerase inhibition leads to a decrease in the CSC subpopulation present in breast and pancreatic tumors cells. Whereas telomerase inhibition by imetelstat had growth inhibitory effects on CSCs as well as bulk tumor cells, CSCs showed a markedly greater degree of growth inhibition than bulk tumor cells. This was supported by observed decreases

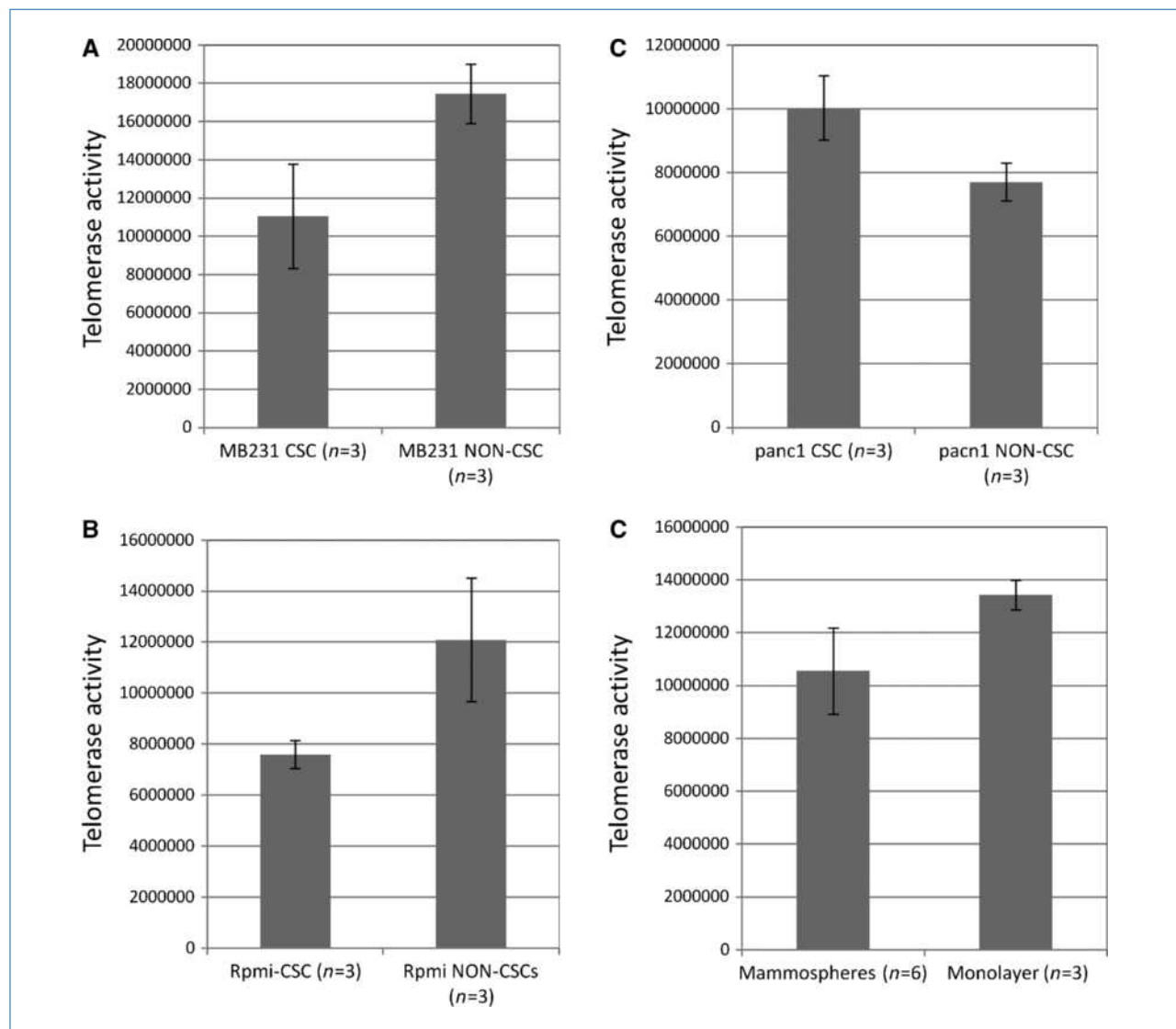


Figure 6. Baseline telomerase activity in CSCs and non-CSCs of MDA MB-231 (A), RPMI-8226 (B), and PANC1 (C) cell lines and between MCF7 mammospheres and monolayer cells (D).

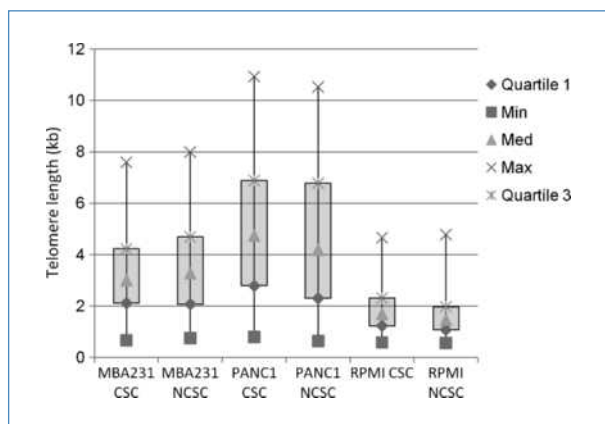


Figure 7. Telomere lengths of CSCs and non-CSCs in three cancer cell lines measured by Universal STELA.

in CSCs in the bulk tumor population after imetelstat treatment and the inhibition of self-renewal in imetelstat-treated MCF7 mammosphere cultures. The *in vitro* effects were likely due to imetelstat-mediated telomerase inhibition because mismatch and sense strand controls, which have no telomerase inhibitory activity, had minimal effects on the growth of MCF7 mammospheres (Fig. 4A). The effect of imetelstat on CSCs is unlikely to be a nonspecific effect of oligonucleotide chemistry, because the separation of growth curves between untreated and imetelstat-treated mammospheres occurred gradually over time.

With telomerase inhibition therapy, a time lag between the start of treatment to the induction of cell senescence or apoptosis is expected, considering the number of divisions a cell must undergo before telomeres become critically short. Whereas imetelstat-mediated telomere shortening was observed in bulk tumors, it is interesting to note that CSC depletion following imetelstat treatment occurred sooner than expected if the CSC inhibitory effects noted occurred solely via a telomere length-based mechanism. Whereas imetelstat treatment did result in telomere shortening (Supplementary Fig. S2) and may have contributed to the effects noted, the data indicate that a non-telomere length-dependent mechanism likely contributed to the activity seen. This is based on two key observations: the rapidity of inhibition of CSC function does not correlate with the time lag one would expect is needed to see telomere shortening sufficient to cause telomere dysfunction. There also was not a clear correlation between baseline telomere length and the sensitivity of CSCs versus bulk tumor cells to imetelstat. The timing of the onset of imetelstat's effects on CSCs suggests several possibilities: first, if a CSC population consists of cells with very short telomeres, the time to reach critically short telomeres would be much shorter than for the bulk tumor cell population. The results presented here indicate that telomere length was not significantly different between CSCs and bulk tumor cells across multiple cell lines. This does not exclude the possibility

that one or a few very short telomeres in CSCs could be responsible, but the universal STELA results do not support this. Our findings are consistent with a recent report on prostate cancer where the investigators were unable to detect a difference in either telomerase activity or telomere length between bulk cells and CSCs (21). In contrast, another report of the sorted CD133+ CSCs from the gliomas of two patients showed remarkably shorter telomeres than the bulk tumors (20). These findings are not unexpected, given the difference in telomerase activity between CSCs and non-CSCs may vary by tissue type and from patient to patient (38, 39). Another possibility is that imetelstat impairs CSC function through as yet undefined telomere shortening-independent pathways. In mouse hair follicle stem cells, mTERT has been shown to have a mTERC-independent function in promoting stem cell proliferation (40). Park and coworkers (41) showed that TERT is an active component in the canonical WNT signaling pathway independent of hTR. hTERT expression and telomerase activity, modulated through GSK3b, are responsible for sustaining gastrointestinal cancer cell survival (42). Flores and coworkers (43) reported that TERT overexpression promoted stem cell mobilization, hair growth, and stem cell proliferation *in vitro* in the absence of changes in telomere length. Masutomi and colleagues reported that hTERT suppression abrogated cell responses to DNA double-stranded breaks and altered the configuration of chromatin independent of telomere maintenance function (44). In agreement with the increasing evidence that TERT has functions other than telomere length maintenance, our data suggest that, whereas treatment with imetelstat does shorten telomeres over time, the effect of imetelstat on CSCs may also involve telomere length-independent pathways. Another possible mechanism for the imetelstat-mediated depletion of CSCs could be through a reversal of the epithelial-mesenchymal transition (EMT). A causal link between EMT and CSCs has been shown (45–47). It was hypothesized by Colitz and colleagues (48) that TERT may play a role in the EMT process based on the observation that cataractogenic EMT in lens epithelial cells was accompanied by an upregulation of estrogen receptor α and increased interaction with TERT. Given the critical roles of telomerase in cell replication and migration, it is important to further investigate a possible link between telomerase, EMT, and CSCs.

In summary, our results show that imetelstat treatment leads to telomerase inhibition and depletion of CSCs from the bulk tumor cells in breast and pancreatic cancer cell lines. CSC-depleted tumor cell populations showed growth inhibition, decreased self-renewal potential and diminished tumorigenic capacity. These findings suggest that telomerase inhibition can inhibit the growth and functionality of CSCs, which are believed to be key drivers of recurrent disease and metastasis in patients. As such, the use of a telomerase inhibitor, particularly when combined with debulking therapy, could have the potential for more durable clinical response in broad tumor types.

Disclosure of Potential Conflicts of Interest

No potential conflicts of interest were disclosed.

Acknowledgments

We thank K.D. Boorsma, S. Edell, and L. Palafox of Geron's Animal Facility for xenograft studies; C.O. Sullivan for help with flow cytometry and cell sorting; S. Gryaznov for valuable advice; I. Ushach and S. dela Llera for technical help; and Lane Eubank for help with the biostatistical analyses.

Grant Support

NCI grant P50 CA127297 (W.E. Wright and J.W. Shay).

The costs of publication of this article were defrayed in part by the payment of page charges. This article must therefore be hereby marked *advertisement* in accordance with 18 U.S.C. Section 1734 solely to indicate this fact.

Received 01/19/2010; revised 08/12/2010; accepted 08/30/2010; published OnlineFirst 11/09/2010.

References

- Bonnet D, Dick JE. Human acute myeloid leukemia is organized as a hierarchy that originates from a primitive hematopoietic cell. *Nat Med* 1997;3:730-7.
- Dick JE. Looking ahead in cancer stem cell research. *Nat Biotechnol* 2009;27:44-6.
- Balic M, Lin H, Young L, et al. Most early disseminated cancer cells detected in bone marrow of breast cancer patients have a putative breast cancer stem cell phenotype. *Clin Cancer Res* 2006;12:5615-21.
- Ponti D, Costa A, Zaffaroni N, et al. Isolation and *in vitro* propagation of tumorigenic breast cancer cells with stem/progenitor cell properties. *Cancer Res* 2005;65:5506-11.
- Collins AT, Berry PA, Hyde C, Stower MJ, Maitland NJ. Prospective identification of tumorigenic prostate cancer stem cells. *Cancer Res* 2005;65:10946-51.
- Singh SK, Hawkins C, Clarke ID, et al. Identification of human brain tumour initiating cells. *Nature* 2004;432:396-401.
- Visvader JE, Lindeman GJ. Cancer stem cells in solid tumours: accumulating evidence and unresolved questions. *Nat Rev Cancer* 2008;8:755-68.
- Vermeulen L, Todaro M, de Sousa Mello F, et al. Single-cell cloning of colon cancer stem cells reveals a multi-lineage differentiation capacity. *Proc Natl Acad Sci U S A* 2008;105:13427-32.
- Li C, Heidt DG, Dalerba P, et al. Identification of pancreatic cancer stem cells. *Cancer Res* 2007;67:1030-7.
- Dean M, Fojo T, Bates S. Tumour stem cells and drug resistance. *Nat Rev Cancer* 2005;5:275-84.
- Donnenberg VS, Donnenberg AD. Multiple drug resistance in cancer revisited: the cancer stem cell hypothesis. *J Clin Pharmacol* 2005;45:872-7.
- Al-Hajj M, Clarke MF. Self-renewal and solid tumor stem cells. *Oncogene* 2004;23:7274-82.
- Harley CB. Telomerase and cancer therapeutics. *Nat Rev Cancer* 2008;8:167-79.
- Herbig U, Jobling WA, Chen BP, Chen DJ, Sedivy JM. Telomere shortening triggers senescence of human cells through a pathway involving ATM, p53, and p21(CIP1), but not p16(INK4a). *Mol Cell* 2004;14:501-13.
- Zhang X, Mar V, Zhou W, Harrington L, Robinson MO. Telomere shortening and apoptosis in telomerase-inhibited human tumor cells. *Genes Dev* 1999;13:2388-99.
- Hahn WC, Stewart SA, Brooks MW, et al. Inhibition of telomerase limits the growth of human cancer cells. *Nat Med* 1999;5:1164-70.
- Dikmen ZG, Gellert GC, Jackson S, et al. *In vivo* inhibition of lung cancer by GRN163L: a novel human telomerase inhibitor. *Cancer Res* 2005;65:7866-73.
- Hochreiter AE, Xiao H, Goldblatt EM, et al. Telomerase template antagonist GRN163L disrupts telomere maintenance, tumor growth, and metastasis of breast cancer. *Clin Cancer Res* 2006;12:3184-92.
- Djojicubrotto MW, Chin AC, Go N, et al. Telomerase antagonists GRN163 and GRN163L inhibit tumor growth and increase chemosensitivity of human hepatoma. *Hepatology* 2005;42:1127-36.
- Marian CO, Cho SK, McEllin BM, et al. The telomerase antagonist, imetelstat, efficiently targets glioblastoma tumor-initiating cells leading to decreased proliferation and tumor growth. *Clin Cancer Res* 2010;16:154-63.
- Marian CO, Wright WE, Shay JW. The effects of telomerase inhibition on prostate tumor-initiating cells. *Int J Cancer* 2010;127:321-31.
- Gryaznov SM, Jackson S, Dikmen G, et al. Oligonucleotide conjugate GRN163L targeting human telomerase as potential anticancer and antimetastatic agent. *Nucleosides Nucleotides Nucleic Acids* 2007;26:1577-9.
- Ju Z, Rudolph KL. Telomeres and telomerase in cancer stem cells. *Eur J Cancer* 2006;42:1197-203.
- Herbert BS, Gellert GC, Hochreiter A, et al. Lipid modification of GRN163, an N3'->P5' thio-phosphoramidate oligonucleotide, enhances the potency of telomerase inhibition. *Oncogene* 2005;24:5262-8.
- Gellert GC, Dikmen ZG, Wright WE, Gryaznov SM, Shay JW. Effects of a novel telomerase inhibitor, GRN163L, in human breast cancer. *Breast Cancer Res Treat* 2006;96:73-81.
- Goldblatt EM, Erickson PA, Gentry ER, Gryaznov SM, Herbert BS. Lipid-conjugated telomerase template antagonists sensitize resistant HER2-positive breast cancer cells to trastuzumab. *Breast Cancer Res Treat* 2009;118:21-32.
- Gomez-Millan J, Goldblatt EM, Gryaznov SM, Mendonca MS, Herbert BS. Specific telomere dysfunction induced by GRN163L increases radiation sensitivity in breast cancer cells. *Int J Radiat Oncol Biol Phys* 2007;67:897-905.
- Li C, Lee CJ, Simeone DM. Identification of human pancreatic cancer stem cells. *Methods Mol Biol* 2009;568:161-73.
- Huang P, Wang CY, Gou SM, Wu HS, Liu T, Xiong JX. Isolation and biological analysis of tumor stem cells from pancreatic adenocarcinoma. *World J Gastroenterol* 2008;14:3903-7.
- Crocker AK, Allan AL. Cancer stem cells: implications for the progression and treatment of metastatic disease. *J Cell Mol Med* 2008;12:374-90.
- Fillmore CM, Kuperwasser C. Human breast cancer cell lines contain stem-like cells that self-renew, give rise to phenotypically diverse progeny and survive chemotherapy. *Breast Cancer Res* 2008;10:R25.
- Kim NW, Piatyszek MA, Prowse KR, et al. Specific association of human telomerase activity with immortal cells and cancer. *Science* 1994;266:2011-5.
- Baird DM, Rowson J, Wynford-Thomas D, Kipling D. Extensive allelic variation and ultrashort telomeres in senescent human cells. *Nat Genet* 2003;33:203-7.
- Xu L, Blackburn EH. Human cancer cells harbor T-stumps, a distinct class of extremely short telomeres. *Mol Cell* 2007;28:315-27.
- Bendix L, Horn PB, Jensen UB, Rubelj I, Kolvråa S. The load of short telomeres, estimated by a new method, Universal STELA, correlates with number of senescent cells. *Aging Cell* 2010;9:383-97.
- Pine SR, Ryan BM, Varticovski L, Robles AI, Harris CC. Microenvironmental modulation of asymmetric cell division in human lung cancer cells. *Proc Natl Acad Sci U S A* 2010;107:2195-200.
- Brennan SK, Wang Q, Tressler R, et al. Telomerase inhibition targets clonogenic multiple myeloma cells through telomere length-dependent and independent mechanisms. *PLoS One* 2010;5.

38. Shervington A, Lu C, Patel R, Shervington L. Telomerase downregulation in cancer brain stem cell. *Mol Cell Biochem* 2009;331:153–9.
39. Zhi L, Yanli H, Jiahua Z, Jinghui Z, Tao H. Determination of telomerase activity in stem cells and non-stem cells of breast cancer. *Frontiers of Med in China*, 2007. 1: 294–98.
40. Sarin KY, Cheung P, Gilson D, et al. Conditional telomerase induction causes proliferation of hair follicle stem cells. *Nature* 2005;436:1048–52.
41. Park JI, Venteicher AS, Hong JY, et al. Telomerase modulates Wnt signalling by association with target gene chromatin. *Nature* 2009; 460:66–72.
42. Mai W, Kawakami K, Shakoori A, et al. Deregulated GSK3 β sustains gastrointestinal cancer cells survival by modulating human telomerase reverse transcriptase and telomerase. *Clin Cancer Res* 2009;15: 6810–9.
43. Flores I, Cayuela ML, Blasco MA. Effects of telomerase and telomere length on epidermal stem cell behavior. *Science* 2005; 309:1253–6.
44. Masutomi K, Possemato R, Wong JM, et al. The telomerase reverse transcriptase regulates chromatin state and DNA damage responses. *Proc Natl Acad Sci U S A* 2005;102:8222–7.
45. Bates RC, Mercurio AM. The epithelial-mesenchymal transition (EMT) and colorectal cancer progression. *Cancer Biol Ther* 2005;4: 365–70.
46. Mani SA, Guo W, Liao MJ, et al. The epithelial-mesenchymal transition generates cells with properties of stem cells. *Cell* 2008;133:704–15.
47. Gupta PB, Onder TT, Jiang G, et al. Identification of selective inhibitors of cancer stem cells by high-throughput screening. *Cell* 2009; 138:645–59.
48. Colitz CM, Sugimoto Y, Lu P, Barden CA, Thomas-Ahner J, Chandler HL. ER α increases expression and interacts with TERT in cataractous canine lens epithelial cells. *Mol Vis* 2009;15:2259–67.

Cancer Research

The Journal of Cancer Research (1916–1930) | The American Journal of Cancer (1931–1940)

The Telomerase Inhibitor Imetelstat Depletes Cancer Stem Cells in Breast and Pancreatic Cancer Cell Lines

Immanual Joseph, Robert Tressler, Ekaterina Bassett, et al.

Cancer Res 2010;70:9494-9504. Published OnlineFirst November 9, 2010.

Updated version	Access the most recent version of this article at: doi: 10.1158/0008-5472.CAN-10-0233
Supplementary Material	Access the most recent supplemental material at: http://cancerres.aacrjournals.org/content/suppl/2010/11/16/0008-5472.CAN-10-0233.DC1

Cited articles	This article cites 46 articles, 14 of which you can access for free at: http://cancerres.aacrjournals.org/content/70/22/9494.full#ref-list-1
-----------------------	--

Citing articles	This article has been cited by 7 HighWire-hosted articles. Access the articles at: http://cancerres.aacrjournals.org/content/70/22/9494.full#related-urls
------------------------	---

E-mail alerts	Sign up to receive free email-alerts related to this article or journal.
----------------------	--

Reprints and Subscriptions	To order reprints of this article or to subscribe to the journal, contact the AACR Publications Department at pubs@aacr.org .
-----------------------------------	--

Permissions	To request permission to re-use all or part of this article, use this link http://cancerres.aacrjournals.org/content/70/22/9494 . Click on "Request Permissions" which will take you to the Copyright Clearance Center's (CCC) Rightslink site.
--------------------	--